

## Multinuclear Gold Complexes

# Synthesis, Structure, Reactivity and Catalytic Implications of a Cationic, Acetylide-Bridged Trigold–JohnPhos Species

Abdessamad Grirrane,<sup>\*,[a]</sup> Eleuterio Álvarez,<sup>[b]</sup> Hermenegildo García,<sup>\*,[a]</sup> and Avelino Corma<sup>\*,[a]</sup>

**Abstract:** The cationic complex [(JohnPhos–Au)<sub>3</sub>(acetylide)] [SbF<sub>6</sub>] (JohnPhos = (2-biphenyl)di-*tert*-butylphosphine, L1) has been characterised structurally and features an acetylide–trigold(I)–JohnPhos system; the trinuclear–acetylide unit, coordinated to the monodentate bulk phosphines, adopts an unprecedented  $\mu, \eta^1, \eta^2, \eta^1$  coordination mode with an additional interaction between distal phenyl rings and gold centres. Other cationic  $\sigma, \pi$ -[[gold(I)L1]<sub>2</sub>] complexes have also been isolated. The reaction of trimethylsilylacetylene with various alcohols (*i*PrOH, *n*BuOH, *n*-HexOH) catalysed by cationic [Au<sup>I</sup>L1][SbF<sub>6</sub>] complexes in CH<sub>2</sub>Cl<sub>2</sub> at 50 °C led to

the formation of acetaldehyde acetals with a high degree of chemo- and regioselectivity. The reaction mechanism was studied, and several organic and inorganic intermediates have been characterised. A comparative study with the analogous cationic [Cu<sup>I</sup>L1][PF<sub>6</sub>] complex revealed different behaviour; the copper metal is lost from the coordination sphere leading to the formation of cationic vinylphosphonium and copper nanoparticles. Additionally, a new catalytic approach for the formation of this high-value cationic vinylphosphonium has been established.

## Introduction

Cationic gold(I) complexes are known as efficient homogeneous catalysts.<sup>[1]</sup> Furthermore, alkynes are some of the most commonly used substrates in gold-catalysed organic synthesis. However, isolable gold–alkyne complexes are rare,<sup>[2]</sup> and the nature of the intermediates involved in these reactions remains uncertain.<sup>[3]</sup> Evidence that gold complexes of terminal alkynes can evolve into polynuclear species has also been provided.<sup>[2d,4]</sup> Recently, the activation of terminal alkynes by Au<sup>I</sup> complexes [L1Au][SbF<sub>6</sub>] (L1 = JohnPhos, (2-biphenyl)di-*tert*-butylphosphine, **A**; Scheme 1) has been reported<sup>[5]</sup> and stable fluxional cationic  $\sigma, \pi$ -digold(I)–JohnPhos phenyl- and alkylacetylide complexes (**B**)<sup>[5a,6]</sup> have been synthesised (Scheme 1, top). In addition, stable fluxional cationic  $\sigma, \pi$ -digold(I)–JohnPhos acetylide complexes (**C**,<sup>[7]</sup> Scheme 1, bottom), prepared when stoichiometric amounts of cationic [L1Au(NCMe)][SbF<sub>6</sub>] complexes react with TMS-acetylene in dry CH<sub>2</sub>Cl<sub>2</sub>, have been isolated and characterised. These digold complexes were as-

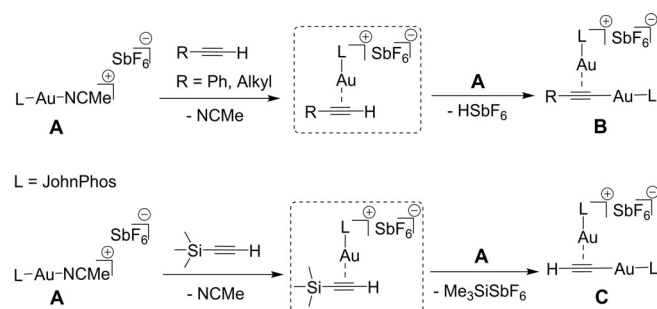
sumed to be formed via a highly reactive cationic  $\pi$ -gold(I)–acetylide complex intermediate. It should be mentioned at this point that the bulky Buchwald-type biarylphosphane ligand (L1) is crucial for stabilising this kind of structure.<sup>[6,7]</sup> The tendency for gold(I) species to form clusters has been shown,<sup>[2d,5a,d,6,8]</sup> and the number of atoms in an Au<sup>I</sup> cluster has been found to influence the stability, properties and catalytic activity of these gold(I) complexes.

Continuing with this research aimed at the characterisation and evaluation of the activity of polynuclear Au<sup>I</sup> complexes, we report herein the incorporation of an additional JohnPhos–Au<sup>+</sup> cation into the HC≡C triple bond of the  $\sigma, \pi$ -acetylide in complexes of the type **C** (Scheme 1), which resulted in a well-defined trinuclear Au<sup>I</sup> complex.

[a] Dr. A. Grirrane, Prof. Dr. H. García, Prof. Dr. A. Corma  
Instituto Universitario de Tecnología Química CSIC-UPV  
Universitat Politècnica de València  
Av. de los Naranjos s/n, 46022 Valencia (Spain)  
E-mail: grirrane@itq.upv.es  
hgarcia@qim.upv.es  
acorma@itq.upv.es

[b] Dr. E. Álvarez  
Departamento de Química Inorgánica  
Instituto de Investigaciones Químicas CSIC-US  
Av. Américo Vespucio 49, 41092 Sevilla (Spain)

Supporting information and the ORCID identification number(s) for the author(s) of this article can be found under:  
<https://doi.org/10.1002/chem.202000420>

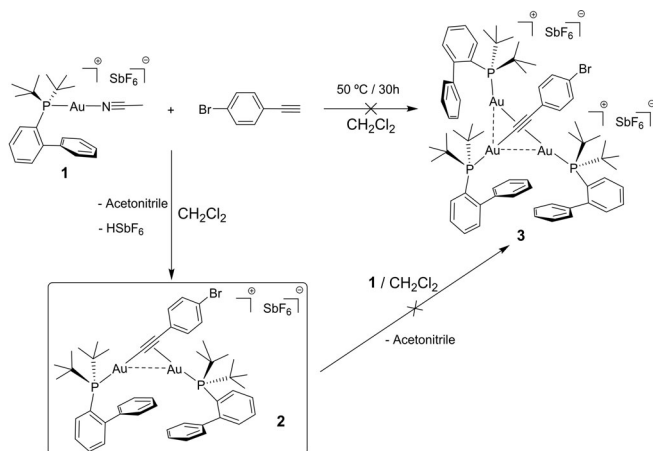


**Scheme 1.** Synthesis of the cationic  $\sigma, \pi$ -digold(I) phenyl- and alkylacetylide ligand L complexes **B** (top) and the cationic  $\sigma, \pi$ -digold(I) acetylide ligand L complexes **C** (bottom).

## Results and Discussion

With this goal, *p*-bromophenylacetylene was treated in the first step with the gold(I)L1 complex **1** in CH<sub>2</sub>Cl<sub>2</sub> at 50 °C for 30 h to yield the isolable fluxional cationic [(σ,π)(L1Au)<sub>2</sub>(μ-bromophenylacetylide)][SbF<sub>6</sub>]<sup>+</sup> complex **2** (Scheme 2) in excellent yield (92%) with the concomitant formation of HSbF<sub>6</sub>. In the second step, an excess of the starting gold(I) complex **1** was added to the cationic σ,π-digold(I) complex **2** and allowed to react for an additional 24 h (Scheme 2). However, under these conditions, it was not possible to obtain the dicationic [(σ,π,π')(L1Au)<sub>3</sub>(μ-bromophenylacetylide)][SbF<sub>6</sub>]<sub>2</sub><sup>+</sup> complex **3** (Scheme 2). It should be mentioned at this point that the direct reaction of a stoichiometric (1:1) mixture of starting gold(I) complex **1** and isolated σ,π-digold(I) complex **2** also failed to form any isolable product. In addition, no evidence for the formation of any new species, including the target [(σ,π,π')(L1Au)<sub>3</sub>(μ-bromophenylacetylide)][SbF<sub>6</sub>]<sub>2</sub><sup>+</sup> complex **3**, could be obtained when CH<sub>2</sub>Cl<sub>2</sub>/isopropanol (1:1) was used as solvent instead of CH<sub>2</sub>Cl<sub>2</sub>. The failure to achieve the incorporation of an additional (L1Au)<sup>+</sup> cation at the free π-coordination position of the C≡C triple bond of the [(σ,π)(L1Au)<sub>2</sub>(μ-bromophenylacetylide)][SbF<sub>6</sub>]<sup>+</sup> complex **2** (Scheme 2) can be explained by electrostatic repulsion of the AuL moieties, or perhaps of the electron density.

The fluxional digold(I) complex **2** was fully characterised by combustion elemental analysis and spectroscopy (see the Experimental Section as well as Figures S1–S6 in the Supporting Information). The <sup>1</sup>H, <sup>31</sup>P, <sup>13</sup>C and DEPT NMR spectra of **2** in CD<sub>2</sub>Cl<sub>2</sub> provide evidence that, under the reaction conditions, the cationic [(σ,π)(L1Au)<sub>2</sub>(μ-bromophenylacetylide)][SbF<sub>6</sub>]<sup>+</sup> complex **2** is the only product formed in detectable amounts (see Figures S1–S4). The <sup>31</sup>P NMR spectrum shows the disappearance of the signal corresponding to initial gold(I) complex **1** at 57.02 ppm (singlet) and the appearance of a new signal at 62.89 ppm (singlet) for **2** (see Figure S4). ESI-MS analysis of a solution obtained after dissolving complex **2** in CH<sub>2</sub>Cl<sub>2</sub> showed an intense positive-ion MS peak at 1171.0 Da (see Figure S5),



**Scheme 2.** Synthesis of the cationic [(σ,π)(L1Au)<sub>2</sub>(μ-bromophenylacetylide)][SbF<sub>6</sub>]<sup>+</sup> complex **2** (first step) and failure to obtain dicationic [(σ,π,π')(L1Au)<sub>3</sub>(μ-bromophenylacetylide)][SbF<sub>6</sub>]<sub>2</sub><sup>+</sup> complex **3** (second step).

which is attributable to the cationic [C<sub>48</sub>H<sub>58</sub>Au<sub>2</sub>BrP<sub>2</sub>]<sup>+</sup> species, the observed peak cluster showing good agreement with the simulated isotopic distribution for the molecular formula C<sub>48</sub>H<sub>58</sub>Au<sub>2</sub>BrP<sub>2</sub> and the fragmentation pattern of the peak can be easily rationalised on the basis of the structure of complex **2**, confirming the elemental composition (see Figure S5). Moreover, the MS peaks recorded in negative-ion mode at 234.3 and 236.3 Da correspond to the two <sup>121</sup>Sb and <sup>123</sup>Sb isotopes of the [SbF<sub>6</sub>]<sup>-</sup> counter anion (see Figure S5). In addition, the HR-ESI-MS peak recorded in positive-ion mode at 1169.2377 amu is in good agreement with the corresponding simulated mass of 1169.2528 amu (see Figure S6 for the isotopic distribution and single mass analysis).

The solid-state structure of [(σ,π)(L1Au)<sub>2</sub>(μ-bromophenylacetylide)][SbF<sub>6</sub>]<sup>+</sup> complex **2** was confirmed by single-crystal X-ray diffraction analysis. An ORTEP diagram of **2** is shown in Figure 1 (for the X-ray diffraction data, ORTEP view and crystal-packing details, see Table S1 and Figure S7 in the Supporting Information).

These results point to the difficulty in obtaining more than dinucleation in gold complexes of the type A (Scheme 1) under our reaction conditions. For this reason, the reactivity of complexes of the type B (Scheme 1) was studied in the second stage of this work. In our previous work,<sup>[7]</sup> we showed that a stoichiometric mixture of trimethylsilylacetylene and gold(I) complex **1** in CH<sub>2</sub>Cl<sub>2</sub>/isopropanol at 45 °C for 24 h leads, in good yield, to the formation of the isolable fluxional cationic σ,π-digold(I)-acetylide complex **4** with concomitant formation of the Me<sub>3</sub>SiSbF<sub>6</sub> salt (Scheme 3, step i). It should be noted that, even when the reaction time and temperature were increased to 50 h and 60 °C, respectively, in the presence of an excess of gold(I) complex **1**, no evidence of any new gold(I) species was obtained, except for the previously formed

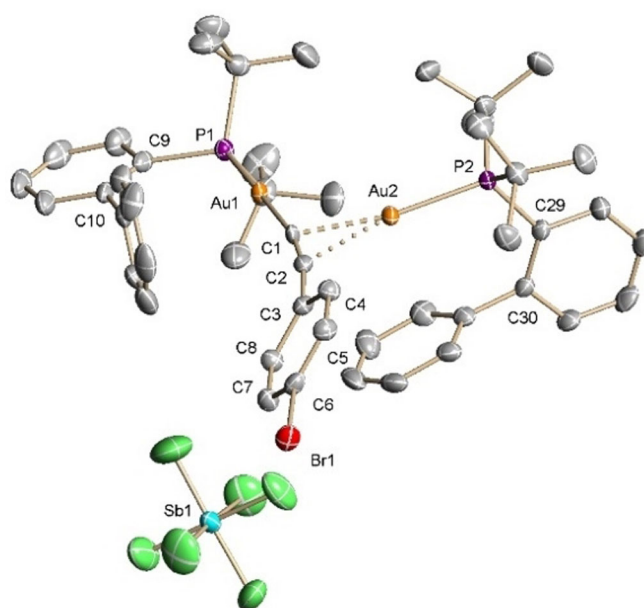


**Figure 1.** ORTEP diagram of cationic [(σ,π)(L1Au)<sub>2</sub>(μ-bromophenylacetylide)][SbF<sub>6</sub>]<sup>+</sup> complex **2**. Hydrogen atoms have been omitted for clarity. Thermal ellipsoids are set at the 30% probability level.

$[(\sigma,\pi)(L1Au)_2(\mu\text{-acetylide})][SbF_6]$  complex **4**. Interestingly, when  $CH_2Cl_2$ /isopropanol (1:1) was used instead of  $CH_2Cl_2$  at  $60^\circ C$  for 48 h, incorporation of an additional  $(L1Au)^+$  cation, replacing the hydrogen atom present in the  $\sigma$ -coordination position of the  $C\equiv C$  triple bond of  $[(\sigma,\pi)(L1Au)_2(\mu\text{-acetylide})][SbF_6]$  complex **4**, was observed, leading to the unusual cationic  $Au_3$  complex **5** (Scheme 3). We suggest that alcohols as amphoteric solvents could abstract the acidic proton present in the acetylide  $HC\equiv C$  fragment of complex **4** and the resulting anionic intermediate nucleophilically attack the  $L1Au^+$  cation of complex **1**. In this way, due to the role of the alcohol,  $[(\sigma,\pi,\sigma')(L1Au)_3(\mu\text{-acetylide})][SbF_6]$  complex **5** is produced with concomitant formation of the strong Brønsted acid  $HSbF_6$  (Scheme 3, step ii).

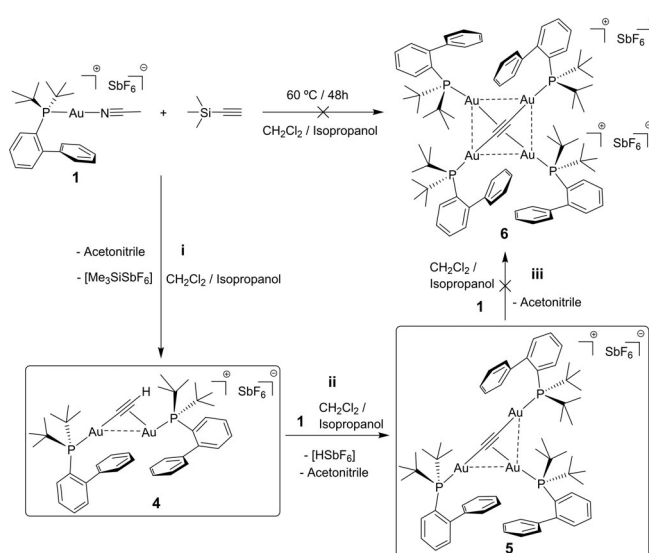
Finally, no evidence for the formation of the tetragold  $[(\sigma,\pi)_2(L1Au)_4(\mu\text{-acetylide})][SbF_6]_2$  complex **6** (Scheme 3) could be obtained, even when the reaction time was increased to 70 h. The failure to incorporate an additional  $L1Au^+$  cation at the free  $\pi$ -coordination position of the  $C\equiv C$  triple bond in the  $[(\sigma,\pi,\sigma')(L1Au)_3(\mu\text{-acetylide})][SbF_6]$  complex **5** (Scheme 5) can be explained by the steric hindrance at this position and the low electron density of the  $C\equiv C$  triple bond linked to three Au atoms.

Trigold(I) complex **5** was fully characterised by combustion elemental analysis and spectroscopy (see the Experimental Section as well as Figures S8–S12 in the Supporting Information). The  $^1H$ ,  $^{31}P$ ,  $^{13}C$ , DEPT and HMQC NMR spectra of **5** in  $CD_2Cl_2$  provide evidence for the formation of the cationic  $[(\sigma,\pi,\sigma')(L1Au)_3(\mu\text{-acetylide})][SbF_6]$  complex **5** under the reaction conditions (Scheme 3). Thus, the  $^{31}P$  NMR spectrum shows the disappearance of the signal corresponding to initial gold(I) complex **1** at 57.02 ppm and the appearance of a new signal at 62.07 ppm for **5** (see Figure S12). The ethynediyl bridge in the  $\sigma,\pi,\sigma'$ -acetylide complex **5** exhibits a unique  $^{13}C$  chemical shift at 153.25 ppm (q,  $^2J_{CP}=47.38$  Hz) due to the fast fluxional-

ity of the three  $L1Au$  fragments (see Figure S9), as confirmed by DEPT and HMQC NMR experiments (see Figures S10 and S11). The ESI-MS of a solution obtained after dissolving complex **5** in  $CH_2Cl_2$  shows only one intense positive-ion MS peak at 1509.5 Da (see Figure S13), which is attributable to the cationic  $[C_{62}H_{81}Au_3P_3]^+$  species. The observed peak cluster is in good agreement with the simulated isotopic distribution for the molecular formula  $C_{62}H_{81}Au_3P_3$  (see Figure S13). The MS peaks recorded in negative-ion mode at 234.7 and 236.6 Da correspond to the two  $^{121}Sb$  and  $^{123}Sb$  isotopes of the  $[SbF_6]^-$  counter anion (see Figure S13) and are also in good accord with the simulated isotopic distribution for the molecular formula  $SbF_6$  (see Figure S13). In addition, the HR-ESI-MS peak recorded in positive ion mode at 1509.4524 amu is in good agreement with the corresponding simulated mass of 1509.4543 amu (see Figure S14 for the isotopic distribution of this signal).

The single-crystal X-ray diffraction structure of the cationic  $[(\sigma,\pi,\sigma')(L1Au)_3(\mu\text{-acetylide})][SbF_6]$  complex **5** is illustrated in Figure 2 and shows that the acetylide bridge coordinates to  $Au_3$  in a  $\eta^1,\eta^2,\eta^1$  fashion (for the X-ray diffraction data, ORTEP view and crystal-packing details, see Table S2 and Figure S15).

To gain information on the chemical properties of complex **5**, the catalysed nucleophilic addition of isopropanol to trimethylsilylacetylene was investigated, the evolution of the reaction mixture being monitored by  $^1H$  and  $^{31}P$  NMR spectroscopy. Special attention was paid to the signals supporting the intermediacy of gold(I)–acetylide complexes **4** and **5**. The spectroscopic study revealed the appearance of another four gold(I) complexes **7–10** as intermediates during the formation of acetaldehyde diisopropyl acetal (**11**) as the final product of this catalytic reaction (see Scheme 4). In these experiments, gold complex **1** (3 mol%) was added to a mixture of TMS-acetylene



**Scheme 3.** Synthesis of cationic digold(I)  $[(\sigma,\pi)(L1Au)_2(\mu\text{-acetylide})][SbF_6]$  complex **4** (step i), cationic trigold(I)  $[(\sigma,\pi,\sigma')(L1Au)_3(\mu\text{-acetylide})][SbF_6]$  complex **5** (step ii) and failure to obtain tetragold  $[(\sigma,\pi)_2(L1Au)_4(\mu\text{-acetylide})][SbF_6]_2$  complex **6** (step iii).

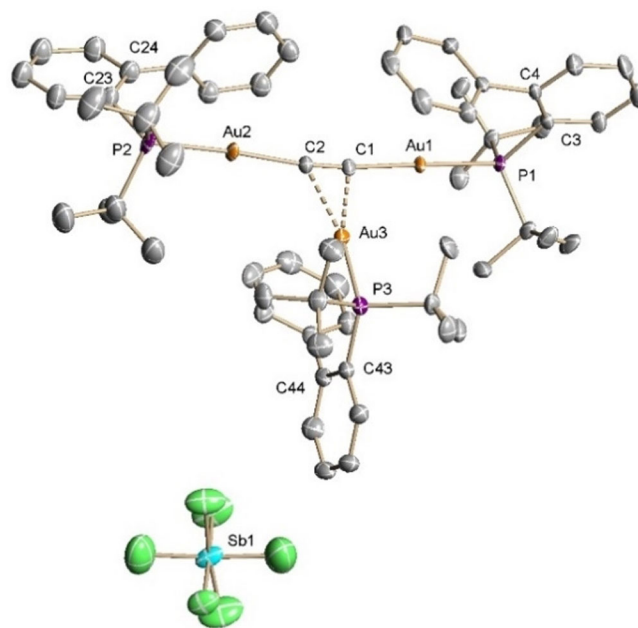
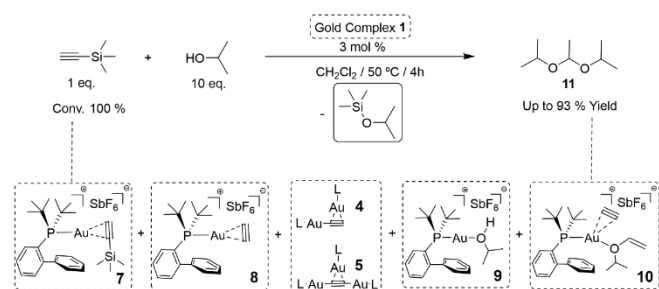


**Figure 2.** ORTEP diagram of cationic  $[(\sigma,\pi,\sigma')(L1Au)_3(\mu\text{-acetylide})][SbF_6]$  complex **5**. Hydrogen atoms have been omitted for clarity. The thermal ellipsoids are set at the 30% probability level.

(1 equiv) and isopropanol (10 equiv) at 50 °C in  $\text{CD}_2\text{Cl}_2$  (Scheme 4). The  $^{31}\text{P}$  NMR spectrum recorded at 10 min reaction time showed new peaks at 58.43 (58%), 61.94 (3%), 62.53 (10%), 64.88 (9%) and 67.88 ppm (5%) attributable, respectively, to the cationic complexes isopropanol–gold(I)L1 **9**,  $\sigma,\pi$ -digold(I)L1–acetylide **4**,  $[(\sigma,\pi,\sigma')(L1\text{Au})_3(\mu\text{-acetylide})][\text{SbF}_6]$  **5**, acetylide–gold(I)L1 **8** and (isopropyl vinyl ether)–gold(I)L1–acetylide **10** together with the peak corresponding to unreacted complex **1** at 57.58 ppm (14%; see Figure S16 in the Supporting Information). After 30 min, the complexes **1** (1.5%), acetylide–gold(I)L1 **8** (3%) and (isopropyl vinyl ether)–gold(I)L1–acetylide **10** (0%) had almost completely disappeared, the percentage of digold(I)L1 **4** (17%) and trigold(I)L1 **5** (50%) in the mixture had increased, and the percentage of isopropanol–gold(I)L1 **9** (19%) had decreased. The formation of 9% of trimethylsilylacetylide–gold(I)L1 complex **7**, characterised by a signal at 63.12 ppm (see Figure S17), was also observed. Moreover, the  $^1\text{H}$  NMR spectrum recorded after 30 min confirmed the coexistence of complexes **4**, **5** and **9** (see Figure S18). The assignments of the gold(I) complexes based on the  $^{31}\text{P}$  NMR signals were firmly supported by HR-ESI-MS analysis of the reaction mixture. Positive-ion MS peaks at  $m/z=1015.3203$  (**4**), 1509.4312 (**5**), 593.2222 (**7**), 521.1672 (**8**), 555.2205 (**9**) and 607.2404 (**10**) were recorded (see Figures S19–S24, respectively). In addition to the exact mass in the HR-ESI-MS, the fragmentation patterns were also in complete accordance with the structures of the gold(I) complexes **4**, **5** and **7–10** (see Figures S19–S24), thereby confirming the formation and composition of these gold(I) complexes as intermediates. High-resolution single-mass analysis of gold(I) intermediates **7** and **10** (Scheme 4) was performed with a tolerance of less than 5 ppm (see Figures S19 and S22).

Regarding the reaction product, acetaldehyde diisopropyl acetal (**11**) was obtained in excellent yield under mild conditions without the need for acid additives (Scheme 4). It has been reported in the literature that the addition of alcohols to alkynes catalysed by gold(I) complexes generally requires a Brønsted acid as co-catalyst.<sup>[11]</sup> GC-MS analysis of **11** ( $\text{C}_8\text{H}_{18}\text{O}_2$ ) dissolved in  $\text{CH}_2\text{Cl}_2$  showed a peak at 146.10 Da, in agreement with the molecular formula (see Figure S25 in the Supporting Information). In addition, (isopropoxy)trimethylsilane ( $\text{C}_6\text{H}_{16}\text{OSi}$ , Scheme 4) was also formed in this reaction by silyla-

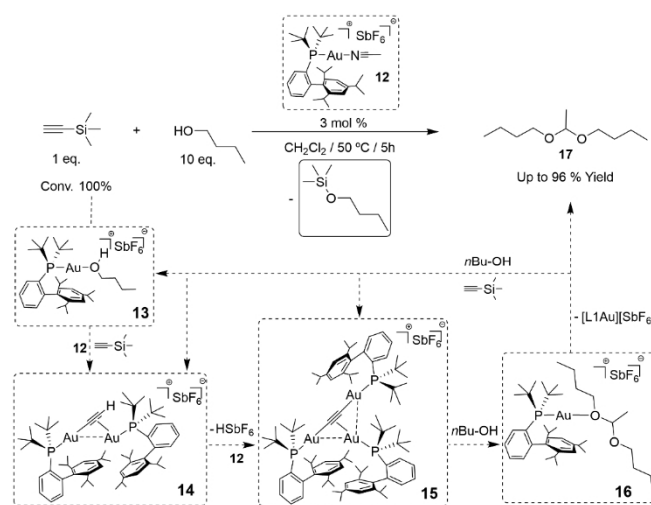


**Scheme 4.** Synthesis of acetaldehyde diisopropyl acetal (**11**) catalysed by cationic gold(I) complex **1** and structures of the  $\text{Au}^{\text{I}}$  intermediates determined by  $^1\text{H}$  and  $^{31}\text{P}$  NMR spectroscopy and HR-ESI-MS.

tion of the OH group of isopropanol; characterisation by GC-MS, showed a peak at 132.1 Da (see Figure S26).

To expand the scope of cationic gold(I) complexes as catalysts and in an attempt to confirm the general mechanism for the addition of alcohols to acetylene, the more bulky cationic L2gold(I) complex **12** and *n*-butanol were used as catalyst and reagent, respectively, instead of cationic L1gold(I) complex **1** and isopropanol (Scheme 5). The course of the reaction was also monitored by  $^{31}\text{P}$  NMR analysis of the reaction mixture, looking for signals of gold(I) intermediates, including butanol adduct **13** and acetylides **14** and **15** as monogold(I), digold(I) and trigold(I) complexes, respectively. Thus, the  $^{31}\text{P}$  NMR spectrum recorded at 30 min reaction time revealed the total consumption of the starting gold(I) complex **12**, which should appear at 55.64 ppm (see Figures S27 and S28 in the Supporting Information for the  $^1\text{H}$  and  $^{31}\text{P}$  NMR spectra of pure complex **12**). New peaks were observed at 56.67 (37%), 62.09 (51%) and 60.26 ppm (5%), attributable to cationic complexes butanol–gold(I)L2 **13**,  $[(\sigma,\pi)(L2\text{Au})_2(\mu\text{-acetylide})][\text{SbF}_6]$  **14**, and  $[(\sigma,\pi,\sigma)(L2\text{Au})_3(\mu\text{-acetylide})][\text{SbF}_6]$  **15**, respectively (see Figure S29). Two additional  $^{31}\text{P}$  peaks at 65.85 (2%) and 56.13 ppm (4%) corresponding, respectively, to acetylide–gold(I)L2 and acetal–gold(I)L2 (**16**) intermediates were also observed (see Figure S29).

Evidence supporting the intermediacy of gold(I) complex **16** (Scheme 5), in which acetal **17** is coordinated to a  $\text{Au}^{\text{I}}$  complex, was provided by HR-ESI-MS of the reaction mixture showing the presence of a positive-ion MS peak at  $m/z=795.4427$ , which can be attributed to the cationic gold complex  $[\text{C}_{39}\text{H}_{67}\text{AuO}_2\text{P}]^+$  (see Figure S30 in the Supporting Information). Release of acetaldehyde dibutyl acetal (**17**) as the final product by ligand exchange with *n*-butanol or TMS-acetylene would lead to the formation of gold complex **13** or **14/15**, respectively, ready to undergo a subsequent catalytic cycle (Scheme 5). Assignment of this series of gold(I) complexes based on the  $^{31}\text{P}$  NMR signals was firmly supported by HR-ESI-MS analysis of



**Scheme 5.** Synthesis of acetaldehyde dibutyl acetal (**17**) catalysed by bulky cationic gold(I) complex **12** and structures of the  $\text{Au}^{\text{I}}$  intermediates determined by  $^1\text{H}$  and  $^{31}\text{P}$  NMR spectroscopy and HR-ESI-MS.

the reaction mixture. Positive-ion MS peaks at  $m/z = 693.3687$  (**13**–2H), 1267.5972 (**14**) and 1887.9171 (**15**) were observed (see Figures S31–S33). The high-resolution single-mass analysis of digold(I) intermediate complex **14** (Scheme 5) is presented with a tolerance of less than 5 ppm in Figure S32.

Acetaldehyde dibutyl acetal (**17**) was also obtained in excellent yield (Scheme 5). GC-MS analysis of **17** ( $C_{10}H_{22}O_2$ ) dissolved in  $CH_2Cl_2$  showed a peak at 174.1 Da, in agreement with the molecular formula (see Figure S34 in the Supporting Information). In addition, (butoxy)trimethylsilane (Scheme 5) was also characterised by GC-MS analysis, based on the peak at 146.1 Da, arising from the silylation of 1-butanol (see Figure S35).

It should be mentioned that a 3:1 mixture of trimethylsilylacetylene and gold(I) complex **12** in  $CH_2Cl_2$  at  $50^\circ C$  for 30 h led to the direct formation of the cationic  $\sigma, \pi$ -(L2Au)<sub>2</sub>-acetylide complex **14** in good yield (91%). The digold(I) complex **14** was fully characterised on the basis of combustion elemental analysis and spectroscopy (see the Experimental Section and Figures S36–S42 in the Supporting Information). The  $^{31}P$  NMR spectrum shows that the signal corresponding to the initial gold(I) complex **12** at 55.64 ppm has shifted to 62.13 ppm due to the formation of complex **14** (see Figure S40). The  $\sigma, \pi$ -acetylide complex **14** exhibits  $^{13}C$  chemical shifts at 140.18 (t,  $^2J_{CP} = 64.21$  Hz) and 96.40 ppm (t,  $^2J_{CP} = 15.60$  Hz; see Figure S37) corresponding to the C and CH moieties of the bridging ethynediyl ( $C\equiv CH$ ), respectively, as confirmed by DEPT and HMQC NMR experiments (see Figures S38 and S39). The ESI-MS of a solution obtained after dissolving complex **14** in  $CH_2Cl_2$  showed only one intense positive-ion MS peak at 1267.4 Da (see Figure S41), which is attributable to the cationic  $[C_{60}H_{91}Au_2P_2]^+$  species. The observed peak cluster is in good agreement with the simulated isotopic distribution for the molecular formula  $C_{60}H_{91}Au_2P_2$ . The fragmentation pattern of this positive-ion MS peak shows an intense peak at 621.1 Da (see Figure S41), which is attributable to the cationic  $L2Au^+$  fragment  $[M-SbF_6^- - L2Au(C\equiv CH)]^+$  (see Figure S41). On the other hand, the negative-ion MS peaks recorded at 234.4 and 236.3 Da corresponding to the two  $^{121}Sb$  and  $^{123}Sb$  isotopes of the  $[SbF_6]^-$  counter anion (see Figure S41) are in good accord with the simulated isotopic distribution for the molecular formula  $SbF_6$  (see Figure S41). The high-resolution single-mass analysis of digold(I) intermediate complex **14** is presented with a tolerance of less than 5 ppm in Figure S42 in the Supporting Information.

The X-ray crystal structure of the cationic  $[(\sigma, \pi)(L2Au)_2(\mu\text{-acetylide})][SbF_6]$  complex **14** is illustrated in Figure 3. As can be seen, the acetylide bridge coordinates to  $Au_2$  in a  $\eta^1, \eta^2$  fashion (for the X-ray diffraction data, ORTEP view and crystal-packing details, see Table S3 and Figure S43 in the Supporting Information).

To verify the catalytic activity and thermal stability of gold(I) catalyst **12**, acetaldehyde dihexyl acetal (**20**) was synthesised in the presence of **12** at  $110^\circ C$  instead of  $50^\circ C$  using *n*-hexanol as reagent (Scheme 6). It has been reported that when  $CH_2Cl_2$  is used as a solvent at high temperatures it can undergo partial decomposition by reacting with alcohol present in

the medium, in this case leading to the formation of 1-(chloromethoxy)hexane, HCl and the subsequent formation of the cationic chloro-bridged digold(I)L2 complex **18** as a less active but more stable intermediate (Scheme 6). The  $^{31}P$  NMR spectrum of the reaction mixture in  $CD_2Cl_2$  recorded at 5 h reaction time provides evidence for the total consumption of the starting gold(I) catalyst **12**, with the formation of the cationic  $[(\sigma, \pi, \sigma')(L2Au)_3(\mu\text{-acetylide})][SbF_6]$  complex **15** (55%), which exhibits a signal at 60.22 ppm. Furthermore, the  $[(\sigma, \pi)(L2Au)_2(\mu\text{-acetylide})][SbF_6]$  complex **14**, characterised by a peak at 62.06 ppm, has been almost completely consumed (1%) and the cationic hexanol-gold(I) adduct **19** appears at 59.11 ppm (19%; see Figure S44 in the Supporting Information). Also, the  $^{31}P$  NMR spectrum shows the disappearance of the signal corresponding to the initial gold(I) complex **12** at 55.64 ppm and the appearance of a new signal at 68.17 ppm (24%) arising from the  $[(L2Au)_2(\mu\text{-Cl})][SbF_6]$  complex **18** (Figure S44). It is

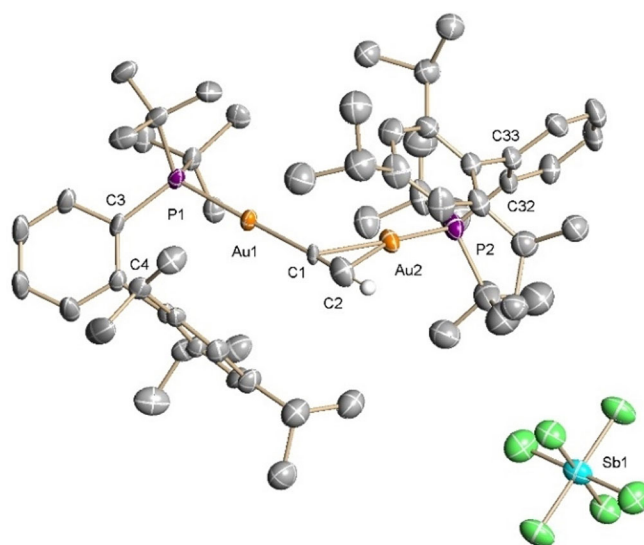
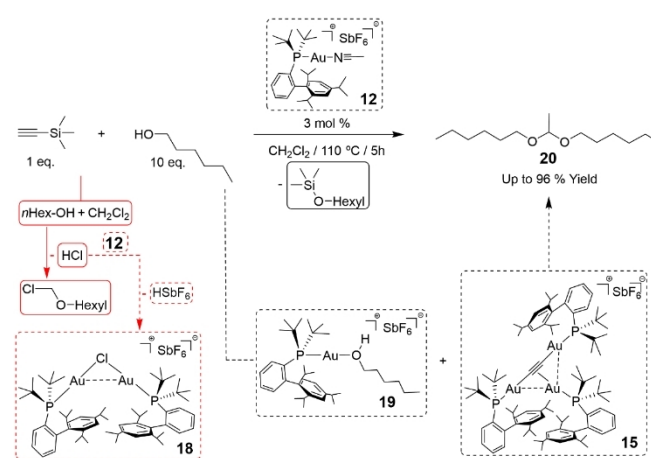


**Figure 3.** ORTEP diagram of cationic  $[(\sigma, \pi)(L2Au)_2(\mu\text{-acetylide})][SbF_6]$  complex **14**. Hydrogen atoms have been omitted for clarity. The thermal ellipsoids are set at the 30% probability level.



**Scheme 6.** Synthesis of acetaldehyde dihexyl acetal (**20**) using bulky cationic gold(I) complex **12** as catalyst in  $CH_2Cl_2$  at  $110^\circ C$  and structures of the  $Au^I$  intermediates determined by  $^1H$  and  $^{31}P$  NMR spectroscopy and HR-ESI-MS.

likely that, at high reaction temperatures, partial deactivation of gold(I) complex **12** occurs due to reaction with chloride ions released into the medium (HCl), resulting in the formation of the less active cationic chloro-bridged digold(I) complex **18**. It should be noted that, when the reaction was performed at 50 °C, no deactivation of the gold(I) catalyst was observed and the solid catalyst could be recovered from the reaction mixture and reused three times without losing activity and selectivity. Furthermore, 1-(chloromethoxy)hexane (Scheme 6) was also formed during this reaction through the partial condensation of *n*-hexanol and CH<sub>2</sub>Cl<sub>2</sub> and characterised by HR-ESI-MS analysis (see Figure S45).

HR-ESI-MS analysis of the Au<sup>I</sup> catalyst recovered from CH<sub>2</sub>Cl<sub>2</sub> showed the presence of a positive-ion MS peak at 1277.5754 Da (see Figure S46 in the Supporting Information), which is attributable to the cationic chloro-bridged digold(I) species [C<sub>58</sub>H<sub>90</sub>Au<sub>2</sub>ClP<sub>2</sub>]<sup>+</sup> species derived from complex **18**.<sup>[8e,9]</sup> The observed peak cluster shows good agreement with the simulated isotopic distribution for the molecular formula C<sub>58</sub>H<sub>90</sub>Au<sub>2</sub>ClP<sub>2</sub> (see Figure S46). The two additional intense positive-ion MS peaks at 721.3954 and 1887.8768 Da are attributable to the cationic monogold(I) hexanol adduct **19** and trigold(I) [(σ,π,σ')(L2Au)<sub>3</sub>(μ-acetylide)][SbF<sub>6</sub>] complex **15**, respectively. The observed peak clusters show good agreement with the simulated isotopic distributions for the molecular formulae of **19** and **15** (see Figures S47 and S48).

The cationic [(L2Au)<sub>2</sub>(μ-Cl)][SbF<sub>6</sub>] complex **18** was also characterised by single-crystal X-ray crystallography (Figure 4), the data showing a chloride bridge coordinating the Au atoms (for the X-ray diffraction data, ORTEP view and crystal-packing details, see Table S4 and Figure S49 in the Supporting Information).

Acetaldehyde dihexyl acetal (**20**) was also obtained in excellent yield (96%) (Scheme 6). GC-MS analysis of **20** dissolved in CH<sub>2</sub>Cl<sub>2</sub> showed a peak at the *m/z* = 230.2, in agreement with the molecular formula (C<sub>14</sub>H<sub>30</sub>O<sub>2</sub>; see Figure S50 in the Supporting Information). Also, high-resolution single-mass analysis of compound **20** was performed with a tolerance of less than 5 ppm; the value of 231.2323 amu < is in good agreement with the molecular formula C<sub>14</sub>H<sub>30</sub>O<sub>2</sub>+H (231.2324 amu; see Figure S51). In addition, (hexoxy)trimethylsilane (Scheme 6), formed as a byproduct during this reaction, was characterised by GC-MS, recording a peak at *m/z* = 174.2, which corresponds to the molecular formula C<sub>9</sub>H<sub>22</sub>OSi (see Figure S52).

At this stage of the work, it was of interest to determine whether the analogous cationic complex [L1Cu<sup>I</sup>][PF<sub>6</sub>]<sup>-</sup> (**21**)<sup>[10]</sup> behaved similarly to the Au<sup>I</sup> complexes in terms of its reactivity with the C≡C triple bond. Aimed at delineating the similarities and differences between Au<sup>I</sup> and Cu<sup>I</sup> complexes, [L1Cu<sup>I</sup>][PF<sub>6</sub>]<sup>-</sup> complex **21** was mixed with trimethylsilylacetylene under the reaction conditions employed for the Au<sup>I</sup> complexes (Scheme 7). Interestingly, no evidence for the formation of any Cu<sup>I</sup>-acetylide complex was obtained. Moreover, completely different behaviour from that of the Au<sup>I</sup> complexes was observed. In this case, cationic vinylphosphonium **22** was isolated in excellent yield (94%) along with copper nanoparticles (Cu NPs; Scheme 7).

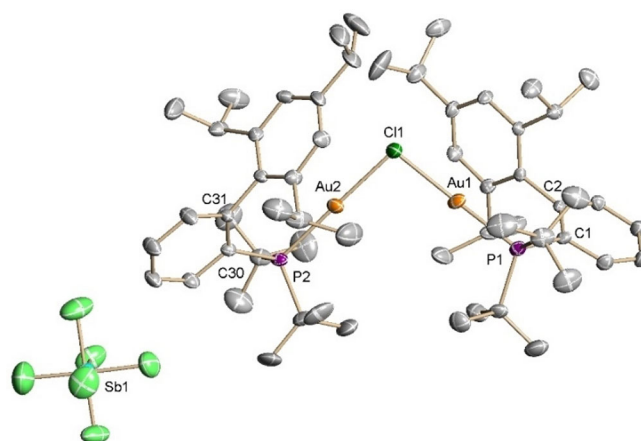
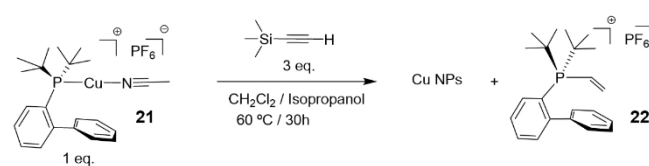


**Figure 4.** ORTEP diagram of cationic [(σ,π)(L2Au)<sub>2</sub>(μ-Cl)][SbF<sub>6</sub>] complex **18**. Hydrogen atoms have been omitted for clarity. The thermal ellipsoids are set at the 30% probability level.

Cationic vinylphosphonium **22** was characterised on the basis of combustion elemental analysis and spectroscopy (see the Experimental Section and Figures S53–S58 in the Supporting Information). The <sup>1</sup>H, <sup>13</sup>C, DEPT, <sup>31</sup>P and <sup>19</sup>F NMR spectroscopic data of **22** in CD<sub>2</sub>Cl<sub>2</sub> provide evidence that, under the reaction conditions (Scheme 7), [(L1)(vinyl)][PF<sub>6</sub>]<sup>-</sup> (**22**) is formed as the final product with concomitant formation of Cu NPs as a red solid precipitate. The <sup>31</sup>P NMR spectrum shows the disappearance of the two signals corresponding to the initial copper(I) complex **21** at 32.49 (singlet) and –144.36 ppm (septuplet for the counter anion, <sup>1</sup>J(PF) = 710.42 Hz.) and the appearance of two new signals, respectively, at 34.98 (singlet) and –144.33 ppm (septuplet) with a relative peak area ratio of 1:1 (see Figure S56). The <sup>1</sup>H NMR spectrum reveals in this case the presence of two doublets for each of the *tert*-butyl methyl groups of compound **22** at 1.23 and 1.47 ppm (see Figure S53). Also, the <sup>19</sup>F NMR spectrum shows a doublet corresponding to the six fluorine atoms of the PF<sub>6</sub><sup>-</sup> counter ion with a coupling constant <sup>1</sup>J(PF) of about 710.46 Hz (see Figure S57). The ESI-MS of a solution obtained after dissolving compound **22** in CH<sub>2</sub>Cl<sub>2</sub> shows only one intense positive-ion MS peak at 325.3 Da (see Figure S58), which is attributable to the cationic species [C<sub>22</sub>H<sub>30</sub>P]<sup>+</sup>. The observed peak cluster shows good agreement with the simulated isotopic distribution for the molecular formula C<sub>22</sub>H<sub>30</sub>P (see Figure S58). On the other hand, a negative-ion MS peak corresponding to the [PF<sub>6</sub>]<sup>-</sup> counter anion was recorded at 144.8 Da (see Figure S58).



**Scheme 7.** Reaction of Cu<sup>I</sup> complex **21** with trimethylsilylacetylene and formation of Cu NPs and cationic vinylphosphonium **22**.

To unambiguously characterise compound **22**, crystals suitable for X-ray diffraction analysis were grown from the reaction mixture after filtration of the red solid precipitate (Cu NPs). Stable crystals of **22** were obtained under ambient conditions. The structure of  $[(L1)(\text{vinyl})][PF_6]$  is illustrated in Figure 5 (for the X-ray diffraction data, ORTEP view and crystal-packing details, see Table S5 and Figure S59 in the Supporting Information). Furthermore, the red precipitate was collected, sonicated in dichloromethane and then analysed by HR-TEM, dark-field STEM, energy-dispersive X-ray spectroscopy and elemental mapping (see Figures S60–S62). The dark-field STEM image is presented in Figure 5. These analyses revealed the formation of well-dispersed Cu NPs with a homogeneous particle size of about 8 nm.

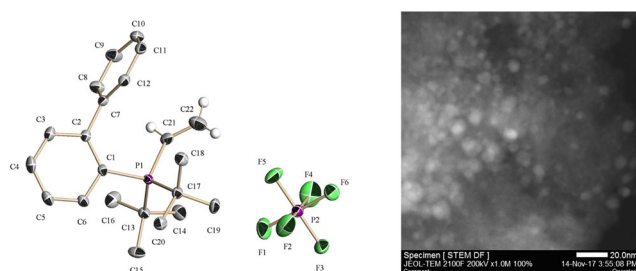
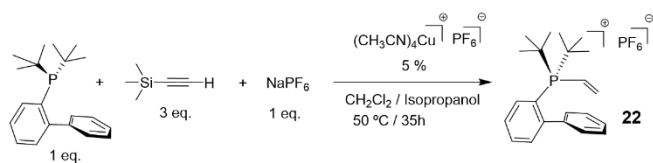


**Figure 5.** ORTEP diagram of  $[(L1)(\text{vinyl})][PF_6]$  compound **22**. Hydrogen atoms have been omitted for clarity. The thermal ellipsoids are set at the 30% probability level (left). Dark-field STEM image of the red precipitate of Cu NPs (right).

Vinylphosphines are key building blocks that undergo ready addition of various nucleophiles (amines,<sup>[11]</sup> phosphines,<sup>[12]</sup> carbanions<sup>[13]</sup>) and other<sup>[14]</sup> reagents to afford functionalised phosphine derivatives, widely used as ligands for advanced catalysts<sup>[15]</sup> and flame retardants<sup>[16]</sup> as well as for the synthesis of conductive nanomaterials.<sup>[17]</sup> However, the synthetic route shown in Scheme 7 and the methods reported in the literature for their synthesis are laborious and require the use of stoichiometric amounts of metals, which does not meet modern environmental requirements.<sup>[18]</sup> Therefore, they cannot be considered as synthetically useful. For this reason, and considering the importance of vinylphosphines, we have elaborated a new catalytic strategy for the synthesis of vinylphosphonium **22** by a facile, one-pot vinylation of tertiary phosphine L1. Mixing  $[Cu(\text{MeCN})_4][PF_6]^{[19]}$  as catalyst (5 mol%) with a stoichiometric amount of L1 (1 equiv), TMS-acetylene (3 equiv) and  $NaPF_6$  (1 equiv) at 50 °C in  $CH_2Cl_2$ /isopropanol (1:1) led to the formation of vinylphosphonium **22** in 96% yield in 35 h (Scheme 8).



**Scheme 8.** One-pot synthesis of cationic vinylphosphonium **22** using a Cu<sup>I</sup> catalyst.

## Conclusion

We have reported herein the isolation of cationic acetylide  $\sigma,\pi$ -digold(I) and  $\sigma,\pi,\sigma'$ -trigold(I) complexes that contain bulky phosphine ligands. The di- and trigold complexes were characterised by single-crystal X-ray diffraction, and their catalytic activity determined in the double addition of alcohols to acetylenes to form acetaldehyde acetals. We propose that the bulk of the phosphine ligands plays a role in the formation of the cationic acetylide  $\sigma,\pi$ -digold(I) and  $\sigma,\pi,\sigma'$ -trigold(I) complexes based on the failure to observe tetragold complexes. Decomposition of dichloromethane was observed at high temperature upon reaction with alcohol with the release of HCl and subsequent formation of a less active cationic chloro-bridged digold(I)-L2 complex. A comparative study with the analogous cationic  $[L1Cu^I][PF_6]$  complex showed remarkably different behaviour, with the decomposition of the complex and the loss of copper metal from the coordination sphere of phosphorus and the formation of a well-characterised cationic vinylphosphonium and copper nanoparticles. A new catalytic route for the formation of vinylphosphonium has been established.

## Experimental Section

The following experimental details are presented in the Supporting Information. 1) The details of the preparation, isolation and full characterisation of the new cationic gold(I) complexes **2**, **5** and **14**, as well as the cationic vinylphosphonium **22**, including the NMR spectra, ESI- and HR-ESI-MS, combustion analysis and single-crystal X-ray crystallography. 2) The details of the preparation, isolation and characterisation of the acetaldehyde acetals **11**, **17** and **20**. 3) HR-ESI-MS and GC-MS data of the intermediate gold(I) complexes **4**, **5**, **7–10**, **13–16**, **18** and **19**. 4) The GC-MS data of (isopropoxy)-, (butoxy)- and (hexoxy)trimethylsilane. 5) The HR-ESI-MS data of 1-(chloromethoxy)hexane. 6) The kinetic measurements determined from NMR and HR-ESI-MS data.

CCDC 1963453 (**2**), 1963454 (**5**), 1963451 (**14**), 1963452 (**18**) and 1963450 (**22**) contain the supplementary crystallographic data for this paper. These data are provided free of charge by The Cambridge Crystallographic Data Centre

All reactions were carried out under argon in solvents dried using a Solvent Purification System (SPS). <sup>1</sup>H NMR spectra were recorded on a Bruker AV300 (300 MHz) spectrometer. The <sup>1</sup>H chemical shifts are reported in ppm using the solvent peak as internal standard ( $CD_2Cl_2$ : 5.27 ppm). The data are reported as follows: Chemical shift (multiplicity (s = singlet, d = doublet, dd = doublet of doublets, t = triplet, q = quadruplet, sept = septuplet, m = multiplet), coupling constants (Hz), assignment). The <sup>13</sup>C chemical shifts were recorded on a Bruker AV300 (300 MHz) spectrometer in ppm using the solvent peak as internal standard ( $CD_2Cl_2$ : 53.84 ppm). The <sup>31</sup>P and <sup>19</sup>F NMR spectra were recorded on a Bruker 300 MHz spectrometer and the <sup>31</sup>P and <sup>19</sup>F chemical shifts are reported in ppm. Gas chromatography (GC) was performed on a Varian 3900 instrument equipped with a TRB-5MS column (5% phenyl, 95% polymethylsiloxane, 30 m, 0.25 mm × 0.25 μm, Teknokroma). GC-MS analyses were performed on an Agilent spectrometer (5973N-6890N) equipped with the same GC column and operated under the same conditions. ESI-MS were acquired on an Agilent Esquire 6000 spectrometer. HR-ESI-MS were recorded on an Waters (XEVO QTOF MS) spectrometer equipped with an ACQUIM UPLC BEH C18 column

(1.7 mm×2.1 mm×100 mm) to obtain the exact mass of the compounds. Elemental analyses were measured on a EuroEA Elemental Analyser Eurovector. HR-TEM was performed with a JEOL JEM-2100F microscope with the field emission gun operating at 200 kV and the images were recorded using a GATAN Orius SC600A.

**Isolation of cationic  $[(\sigma,\pi)(L1Au)_2(\mu\text{-bromophenylacetylide})][SbF_6]$  complex 2:** A mixture of complex  $[Au(L1)(CH_3CN)][SbF_6]$  (**1**; 0.116 g, 0.15 mmol) and *p*-bromophenylacetylene (0.0543 g, 0.30 mmol) was dissolved in dichloromethane (2 mL). The solution was stirred at 50 °C under argon atmosphere for 30 h. Then, the resulting mixture was diluted with  $CH_2Cl_2$  (2 mL), filtered and the supernatant was covered carefully with a layer of *n*-hexane (1.5 mL). A colourless crystalline material corresponding to complex **2**, suitable for single-crystal X-ray crystallography, was obtained upon standing for 48 h at −30 °C. The crystals were collected by filtration, washed with *n*-hexane and dried under vacuum (0.195 g, 93 % yield).  $^1H$  NMR (300 MHz,  $CD_2Cl_2$ ):  $\delta$  = 7.90–7.77 (m, 2H; ArH), 7.60–7.45 (m, 6H; ArH), 7.35–7.15 (m, 10H; ArH), 7.13–7.00 (m, 4H; ArH), 1.39 (s, 18H; *t*Bu  $CH_3$ ), 1.34 ppm (s, 18H; *t*Bu  $CH_3$ );  $^{13}C$  NMR (75 MHz,  $CD_2Cl_2$ ):  $\delta$  = 149.74, 149.55, 143.25, 143.16, 134.43, 134.36, 134.33, 133.76, 133.66, 132.49, 131.59, 129.81, 129.49, 128.40, 128.00, 127.90, 125.78, 125.18, 124.95, 120.39, 38.56, 38.24, 31.32, 31.23 ppm; DEPT-135 NMR (75 MHz,  $CD_2Cl_2$ , +ve):  $\delta$  = 134.43, 134.33, 133.76, 133.65, 132.49, 131.59, 129.81, 129.49, 128.41, 128.00, 127.91, 31.32, 31.23 ppm;  $^{31}P$  NMR ( $CD_2Cl_2$ ):  $\delta$  = 62.89 ppm (s, phosphine ligands); MS (ESI, +ve):  $m/z$ : 1171.0  $[M-SbF_6]^{+}$ ; MS (ESI, −ve):  $m/z$ : 234.3, 236.3  $[SbF_6]^{-}$ ; HRMS (ESI, +ve):  $m/z$  calcd for  $[M-SbF_6]^{+}$ : 1169.2528; found: 1169.2377; elemental analysis calcd (%) for  $C_{48}H_{58}Au_2BrF_6P_2Sb$ : C 40.99, H 4.16; found: C 40.94, H 4.22.

**Isolation of cationic  $[(\sigma,\pi,\sigma)(L1Au)_3(\mu\text{-acetylide})][SbF_6]$  complex 5:** A mixture of complex  $[Au(L1)(CH_3CN)][SbF_6]$  (**1**; 0.077 g, 0.10 mmol) and ethynyltrimethylsilane (0.0294 g, 0.30 mmol) was dissolved in dichloromethane/isopropanol (1:1, 2 mL). The solution was stirred at 60 °C under argon atmosphere for 48 h. Then, the resulting mixture was diluted with  $CH_2Cl_2$ /isopropanol (1:1, 2 mL). A colourless crystalline material corresponding to complex **5**, suitable for single-crystal X-ray crystallography, was obtained upon standing for 30 h at RT. The crystals were collected by filtration, washed with cold *n*-hexane and dried under vacuum (0.161 g, 92 % yield).  $^1H$  NMR (300 MHz,  $CD_2Cl_2$ ):  $\delta$  = 7.92–7.78 (m, 3H; ArH), 7.59–7.43 (m, 7H; ArH), 7.38–7.15 (m, 12H; ArH), 7.12–7.00 (m, 5H; ArH), 1.40 (s, 9H; *t*Bu  $CH_3$ ), 1.35 ppm (s, 9H; *t*Bu  $CH_3$ );  $^{13}C$  NMR (75 MHz,  $CD_2Cl_2$ ):  $\delta$  = 153.25 (q;  $\mu\text{-C}\equiv\text{C}$ ), 150.38, 150.19, 142.94, 142.86, 134.80, 134.78, 133.55, 133.45, 130.99, 130.97, 129.50, 129.44, 129.19, 128.34, 127.48, 127.40, 127.20, 126.65, 38.27, 37.97, 31.27, 31.18 ppm; DEPT-135 NMR (75 MHz,  $CD_2Cl_2$ , +ve):  $\delta$  = 134.80, 134.78, 133.54, 133.44, 130.99, 130.96, 129.50, 129.44, 129.18, 128.34, 127.49, 127.40, 31.27, 31.18 ppm;  $^{31}P$  NMR ( $CD_2Cl_2$ ):  $\delta$  = 62.07 ppm (s, phosphine ligands); MS (ESI, +ve):  $m/z$ : 1509.5  $[M-SbF_6]^{+}$ ; MS (ESI, −ve):  $m/z$ : 234.7, 236.7  $[SbF_6]^{-}$ ; HRMS (ESI, +ve):  $m/z$  calcd for  $[M-SbF_6]^{+}$ : 1509.4524; found: 1509.4543; elemental analysis calcd (%) for  $C_{62}H_{81}Au_3F_6P_3Sb$ : C 42.65, H 4.68; found: C 42.63, H 4.70.

**Isolation of cationic  $[(\sigma,\pi)(L2Au)_2(\mu\text{-acetylide})][SbF_6]$  complex 14:** A mixture of complex  $[Au(L2)(CH_3CN)][SbF_6]$  (**12**; 0.0898 g, 0.10 mmol) and ethynyltrimethylsilane (0.0294 g, 0.30 mmol) was dissolved in dichloromethane (2 mL). The solution was stirred at 60 °C under argon atmosphere for 65 h. Then, the resulting mixture was diluted with  $CH_2Cl_2$  (2 mL), filtered and the supernatant was covered carefully with a layer of *n*-hexane (1.5 mL). A colourless crystalline material corresponding to complex **14**, suitable for single-crystal X-ray crystallography, was formed upon standing for 48 h at −30 °C. The solid was collected by filtration, washed with

cold *n*-hexane and dried under vacuum (0.137 g, 91 % yield).  $^1H$  NMR (300 MHz,  $CD_2Cl_2$ ):  $\delta$  = 7.95–7.75 (m, 2H; ArH), 7.60–7.45 (m, 4H; ArH), 7.20–7.09 (m, 2H; ArH), 7.06–6.90 (s, 4H; ArH), 2.86 (sept, 2H; *i*PrCH), 2.29 (sept, 4H; *i*PrCH), 1.47 (s, 1H;  $\mu\text{-C}\equiv\text{CH}$ ), 1.38 (s, 18H; *t*Bu  $CH_3$ ), 1.32 (s, 18H; *t*Bu  $CH_3$ ), 1.26 (d, 12H; *i*PrCH $_3$ ), 1.16 (d, 12H; *i*PrCH $_3$ ), 0.85 ppm (d, 12H; *i*PrCH $_3$ );  $^{13}C$  NMR (75 MHz,  $CD_2Cl_2$ ):  $\delta$  = 150.02, 147.61, 140.18 (t;  $\mu\text{-C}\equiv\text{CH}$ ), 137.32, 137.24, 135.50, 135.38, 131.43, 128.68, 128.64, 128.07, 127.67, 127.57, 122.37, 96.40 (t;  $\mu\text{-C}\equiv\text{CH}$ ), 39.15, 38.83, 34.35, 31.66, 31.58, 31.21, 25.97, 25.30, 24.40, 23.51 ppm; DEPT-135 NMR (75 MHz,  $CD_2Cl_2$ , +ve):  $\delta$  = 135.49, 135.38, 131.45, 127.67, 127.57, 122.37, 34.35, 31.66, 31.57, 31.21, 25.98, 25.31, 24.41, 23.51 ppm;  $^{31}P$  NMR ( $CDCl_3$ ):  $\delta$  = 62.13 ppm (s, phosphine ligands); MS (ESI, +ve):  $m/z$ : 1267.4  $[M-SbF_6]^{+}$ ; MS (ESI, −ve):  $m/z$ : 234.4, 236.4  $[SbF_6]^{-}$ ; HRMS (ESI, +ve):  $m/z$  calcd for  $[M-SbF_6]^{+}$ : 1267.5927; found: 1267.5972; elemental analysis calcd (%) for  $C_{60}H_{91}Au_2F_6P_2Sb$ : C 47.92, H 6.10; found: C 47.89, H 6.08.

#### Isolation of cationic $[(L1)(vinyl)][SbF_6]$ compound 22

**Method A:** A mixture of complex  $[Cu(L1)(CH_3CN)][PF_6]$  (**21**; 0.0822 g, 0.15 mmol) and ethynyltrimethylsilane (0.0441 g, 0.45 mmol) was dissolved in dichloromethane/isopropanol (1:1, 2 mL). The solution was stirred at 60 °C under argon atmosphere for 30 h. Then, the resulting mixture was diluted with  $CH_2Cl_2$ /isopropanol (1:1, 2 mL) and the suspension filtered to remove the red solid precipitate (Cu NPs). A colourless crystalline material corresponding to complex **22**, suitable for single-crystal X-ray crystallography, was obtained upon standing the supernatant for 30 h at RT. The crystals were collected by filtration, washed with cold *n*-hexane and dried under vacuum (0.065 g, 93 % yield).

**Method B:** A mixture of phosphine L1 (0.0447 g, 0.15 mmol),  $NaPF_6$  (0.026 g, 0.15 mmol), ethynyltrimethylsilane (0.0441 g, 0.45 mmol) and  $[Cu(CH_3CN)_4][PF_6]$  (0.0028 g, 0.0075 mmol) as catalyst (Cu/L1 ratio, 5 mol%) was suspended in  $CH_2Cl_2/CH_3OH$  (1:1, 2 mL). The solution was stirred at 60 °C under argon atmosphere for 35 h. Then, the resulting mixture was diluted with  $CH_2Cl_2/CH_3OH$  (1:1, 2 mL), filtered and the supernatant covered carefully with a layer of *n*-hexane (1 mL). A colourless crystalline material corresponding to compound **22**, suitable for single-crystal X-ray crystallography, was obtained upon standing the supernatant for 30 h at RT. The crystals were collected by filtration, washed with cold *n*-hexane and dried under vacuum (0.067 g, 95 % yield).  $^1H$  NMR (300 MHz,  $CD_2Cl_2$ ):  $\delta$  = 7.95–7.80 (m, 1H; ArH), 7.79–7.65 (m, 1H; vinyl-H), 7.60–7.40 (m, 4H; ArH), 7.37–7.08 (m, 4H; ArH), 5.94–5.65 (m, 1H; vinyl-H), 5.61–5.33 (m, 1H; vinyl-H), 1.47 (d, 9H; *t*Bu  $CH_3$ ), 1.23 ppm (d, 9H; *t*Bu  $CH_3$ );  $^{13}C$  NMR (75 MHz,  $CD_2Cl_2$ ):  $\delta$  = 149.22, 140.55, 135.57, 134.51, 134.22, 134.00, 132.18, 130.16, 129.72, 128.61, 128.34, 128.15, 117.04, 113.28, 37.68, 35.33, 30.64, 28.82 ppm; DEPT-135 NMR (75 MHz,  $CD_2Cl_2$ , +ve):  $\delta$  = 134.51, 134.22, 134.00, 132.18, 130.16, 129.73, 128.61, 128.34, 128.15, 113.25, 30.64, 28.82 ppm; DEPT-135 NMR (75 MHz,  $CD_2Cl_2$ , −ve):  $\delta$  = 135.55 ppm;  $^{31}P$  NMR ( $CDCl_3$ ):  $\delta$  = 62.13 (s, phosphine), 144.34 ppm (sept,  $PF_6^{-}$ );  $^{19}F$  NMR ( $CD_2Cl_2$ ):  $\delta$  = 73.14 ppm (d,  $PF_6^{-}$ ); MS (ESI, +ve):  $m/z$ : 325.3  $[M-PF_6]^{+}$ ; MS (ESI, −ve):  $m/z$ : 144.8  $[PF_6]^{-}$ ; elemental analysis calcd (%) for  $C_{22}H_{30}F_6P_2$ : C 56.17, H 6.43; found: C 56.13, H 6.40.

**General procedure for the catalytic one-pot double addition of alcohols to acetylene—preparation of acetaldehyde acetals **11**, **17** and **20**:** A mixture of isopropanol, butanol or hexanol (2.5 mmol), respectively, with TMS-acetylene (0.25 mmol) and gold(I) complex **1** or **12** (0.0075 mmol) as catalyst (Au/alkyne ratio, 3 mol%) was suspended in  $CH_2Cl_2$  (1 mL), then the flask was evacuated under vacuum and refilled with argon. The evacuation/refilling cycle was repeated three times (pressure 3 bar). The mixture

was stirred at 50 °C for the required time to obtain the maximum yield of acetaldehyde acetals **11**, **17** and **20** compounds (see manuscript). Then, cold *n*-hexane was added to the reaction mixture, the suspension was filtered and the solvents removed under reduced pressure to provide the target acetaldehyde acetals as colourless liquids in yields higher than 93% (see manuscript). The purity and structures of the acetaldehyde acetals **11**, **17** and **20** were confirmed by GC, GC-MS and HR-ESI-MS spectrometry analysis. Compound **11**: GC-MS: *m/z*: 146.1 [M]<sup>+</sup>. Compound **17**: GC-MS: *m/z*: 174.1 [M]<sup>+</sup>. Compound **20**: GC-MS: *m/z*: 230.2 [M]<sup>+</sup>; HR-ESI-MS: *m/z* calcd for [M+1]<sup>+</sup>: 231.2324; found: 231.2323.

## Acknowledgements

Financial support by the Spanish Ministry of Economy and Competitiveness (Severo Ochoa and RTI2018-89027-CO2-R1) and the Generalitat Valenciana (Prometeo 2013–2014) is gratefully acknowledged.

## Conflict of interest

The authors declare no conflict of interest.

**Keywords:** acetals · gold · homogeneous catalysis · multinuclear complexes · phosphorus · reaction mechanisms

- [1] a) A. S. K. Hashmi, G. J. Hutchings, *Angew. Chem. Int. Ed.* **2006**, *45*, 7896–7936; *Angew. Chem.* **2006**, *118*, 8064–8105; b) A. Arcadi, *Chem. Rev.* **2008**, *108*, 3266–3325; c) S. Díez-González, N. Marion, S. P. Nolan, *Chem. Rev.* **2009**, *109*, 3612–3676; d) D. J. Gorin, B. D. Sherry, F. D. Toste, *Chem. Rev.* **2008**, *108*, 3351–3378; e) A. Fürstner, P. W. Davies, *Angew. Chem. Int. Ed.* **2007**, *46*, 3410–3449; *Angew. Chem.* **2007**, *119*, 3478–3519; f) D. Pflästerer, A. S. K. Hashmi, *Chem. Soc. Rev.* **2016**, *45*, 1331–1367; g) L. Prati, A. Villa, *Acc. Chem. Res.* **2014**, *47*, 855–863; h) A. S. K. Hashmi, *Chem. Rev.* **2007**, *107*, 3180–3211; i) A. S. K. Hashmi, *Acc. Chem. Res.* **2014**, *47*, 864–876; j) J. H. Teles, S. Brode, M. Chabanas, *Angew. Chem. Int. Ed.* **1998**, *37*, 1415–1418; *Angew. Chem.* **1998**, *110*, 1475–1478; k) A. S. K. Hashmi, L. Schwarz, J.-H. Choi, T. M. Frost, *Angew. Chem. Int. Ed.* **2000**, *39*, 2285–2288; *Angew. Chem.* **2000**, *112*, 2382–2385; l) A. S. K. Hashmi, T. M. Frost, J. W. Bats, *J. Am. Chem. Soc.* **2000**, *122*, 11553–11554.
- [2] a) P. Schulte, U. Behrens, *Chem. Commun.* **1998**, 1633–1634; b) N. D. Shapiro, F. D. Toste, *Proc. Natl. Acad. Sci. USA* **2008**, *105*, 2779–2782; c) J. Wu, P. Kroll, H. V. R. Dias, *Inorg. Chem.* **2009**, *48*, 423–425; d) T. N. Hooper, M. Green, C. A. Russell, *Chem. Commun.* **2010**, *46*, 2313–2315; e) V. Lavallo, G. D. Frey, S. Kousar, B. Donnadieu, G. Bertrand, *Proc. Natl. Acad. Sci. USA* **2007**, *104*, 13569–13573.
- [3] a) G. Seidel, R. Mynott, A. Fuerstner, *Angew. Chem. Int. Ed.* **2009**, *48*, 2510–2513; *Angew. Chem.* **2009**, *121*, 2548–2551; b) D. Benitez, N. D. Shapiro, E. Tkatchouk, Y. Wang, W. A. Goddard III, F. D. Toste, *Nat. Chem.* **2009**, *1*, 482–486, S482/481–S482/486; c) A. S. K. Hashmi, *Angew. Chem. Int. Ed.* **2010**, *49*, 5232–5241; *Angew. Chem.* **2010**, *122*, 5360–5369.
- [4] a) M. C. Blanco, J. Camara, M. C. Gimeno, P. G. Jones, A. Laguna, J. M. Lopez-de-Luzuriaga, M. E. Olmos, M. D. Villacampa, *Organometallics* **2012**, *31*, 2597–2605; b) I. Braun, A. M. Asiri, A. S. K. Hashmi, *ACS Catal.* **2013**, *3*, 1902–1907; c) X. Zhao, M. Rudolph, A. S. K. Hashmi, *Chem. Commun.* **2019**, *55*, 12127–12135.
- [5] a) A. Grirrane, H. Garcia, A. Corma, E. Alvarez, *ACS Catal.* **2011**, *1*, 1647–1653; b) B. Rubial, A. Ballesteros, J. M. Gonzalez, *Adv. Synth. Catal.* **2013**, *355*, 3337–3343; c) A. Simonneau, F. Jaroschik, D. Lesage, M. Karanik, R. Guillot, M. Malacria, J.-C. Tabet, J.-P. Goddard, L. Fensterbank, V. Gandon, Y. Gimbert, *Chem. Sci.* **2011**, *2*, 2417–2422; d) R. E. M. Brooner, R. A. Widenhoefer, *Angew. Chem. Int. Ed.* **2013**, *52*, 11714–11724; *Angew. Chem.* **2013**, *125*, 11930–11941.
- [6] A. Grirrane, H. Garcia, A. Corma, E. Alvarez, *Chem. Eur. J.* **2013**, *19*, 12239–12244.
- [7] A. Grirrane, E. Alvarez, H. Garcia, A. Corma, *Chem. Eur. J.* **2017**, *23*, 2792–2801.
- [8] a) H. Schmidbaur, A. Hamel, N. W. Mitzel, A. Schier, S. Nogai, *Proc. Natl. Acad. Sci. USA* **2002**, *99*, 4916–4921; b) H. E. Abdou, A. A. Mohamed, J. P. Fackler, Jr., *Inorg. Chem.* **2005**, *44*, 166–168; c) A. Escalle, G. Mora, F. Gagosz, N. Mezailles, X. F. Le Goff, Y. Jean, P. Le Floch, *Inorg. Chem.* **2009**, *48*, 8415–8422; d) A. S. K. Hashmi, T. Lauterbach, P. Noesel, M. H. Vilhelmsen, M. Rudolph, F. Rominger, *Chem. Eur. J.* **2013**, *19*, 1058–1065; e) A. Grirrane, E. Alvarez, H. Garcia, A. Corma, *Angew. Chem. Int. Ed.* **2014**, *53*, 7253–7258; *Angew. Chem.* **2014**, *126*, 7381–7386.
- [9] a) A. S. K. Hashmi, M. C. Blanco, E. Kurpejovic, W. Frey, J. W. Bats, *Adv. Synth. Catal.* **2006**, *348*, 709–713; b) R. Uson, A. Laguna, M. V. Castrillo, *Synth. React. Inorg. Met.-Org. Chem.* **1979**, *9*, 317–324; c) A. Bayler, A. Bauer, H. Schmidbaur, *Chem. Ber./Recl.* **1997**, *130*, 115–118.
- [10] A. Grirrane, E. Alvarez, H. Garcia, A. Corma, *Chem. Eur. J.* **2014**, *20*, 14317–14328.
- [11] a) A. M. Maj, K. M. Pietrusiewicz, I. Suisse, F. Agbossou, A. Mortreux, *J. Organomet. Chem.* **2001**, *626*, 157–160; b) M. S. Rahman, M. Oliana, K. K. Hii, *Tetrahedron: Asymmetry* **2004**, *15*, 1835–1840; c) D. V. Griffiths, H. J. Groombridge, P. M. Mahoney, S. P. Swetnam, G. Walton, D. C. York, *Tetrahedron* **2005**, *61*, 4595–4600.
- [12] a) P. Barbaro, C. Bianchini, G. Giambastiani, A. Togni, *Chem. Commun.* **2002**, 2672–2673; b) M. Alajarin, C. Lopez-Leonardo, P. Llamas-Lorente, *Lett. Org. Chem.* **2004**, *1*, 145–147; c) L.-B. Han, C.-Q. Zhao, *J. Org. Chem.* **2005**, *70*, 10121–10123.
- [13] a) K. M. Pietrusiewicz, M. Zablocka, *Tetrahedron Lett.* **1988**, *29*, 937–940; b) R. T. Paine, E. M. Bond, S. Parveen, N. Donhart, E. N. Duesler, K. A. Smith, H. Noeth, *Inorg. Chem.* **2002**, *41*, 444–448.
- [14] a) K. M. Pietrusiewicz, W. Holody, M. Koprowski, S. Cicchi, A. Goti, A. Brandi, *Phosphorus Sulfur Silicon Relat. Elem.* **1999**, *144–146*, 389–392; b) A. R. Katritzky, M. Piffli, H. Lang, E. Anders, *Chem. Rev.* **1999**, *99*, 665–722; c) K.-W. Tan, F. Liu, Y. Li, G.-K. Tan, P.-H. Leung, *J. Organomet. Chem.* **2006**, *691*, 4753–4758.
- [15] a) Q. Dai, W. Gao, D. Liu, L. M. Kapes, X. Zhang, *J. Org. Chem.* **2006**, *71*, 3928–3934; b) D. Benito-Garagorri, J. Wiedermann, M. Pollak, K. Mereiter, K. Kirchner, *Organometallics* **2007**, *26*, 217–222.
- [16] a) G. Ribera, L. A. Mercado, M. Galia, V. Cadiz, *J. Appl. Polym. Sci.* **2006**, *99*, 1367–1373; b) G. V. Plotnikova, S. F. Malysheva, N. K. Gusarova, A. K. Khaliulin, V. P. Udilov, K. L. Kuznetsov, *Russ. J. Appl. Chem.* **2008**, *81*, 304–309.
- [17] a) S. P. Gubin, N. A. Kataeva, G. B. Khomutov, *Russ. Chem. Bull.* **2005**, *54*, 827–852; b) H. Liu, J. S. Owen, A. P. Alivisatos, *J. Am. Chem. Soc.* **2007**, *129*, 305–312.
- [18] a) S. F. Malysheva, N. K. Gusarova, N. Y. A. Belogorlova, T. V. Kashik, L. B. Krivdin, S. V. Fedorov, B. A. Trofimov, *Phosphorus Sulfur Silicon Relat. Elem.* **2010**, *185*, 1838–1844; b) K. M. Pietrusiewicz, *Phosphorus Sulfur Silicon Relat. Elem.* **1996**, *109–110*, 573–576; c) S. F. Malysheva, N. K. Gusarova, N. A. Belogorlova, A. V. Afonin, S. N. Arbutova, B. A. Trofimov, *Russ. Chem. Bull.* **1997**, *46*, 1799–1801.
- [19] S. F. Rach, F. E. Kuehn, *Chem. Rev.* **2009**, *109*, 2061–2080.

Manuscript received: January 24, 2020  
Version of record online: ■■■■■ 0000

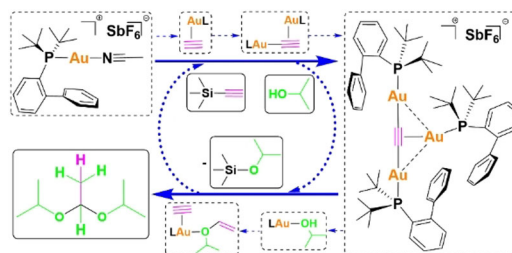
## FULL PAPER

### Multinuclear Gold Complexes

A. Girrane,\* E. Álvarez, H. García,\*  
A. Corma\*



 **Synthesis, Structure, Reactivity and Catalytic Implications of a Cationic, Acetylide-Bridged Trigold–JohnPhos Species**



**Multinuclear gold:** A new family of tri-Au<sup>I</sup> complexes have been characterised as intermediates during the [Au<sup>I</sup>L][SbF<sub>6</sub>]<sup>+</sup> catalytic preparation of acetaldehyde acetals. These well-characterised cation-

ic Au<sup>I</sup> intermediates lend support to the proposed reaction mechanism. An analogous copper complex revealed different behaviour, leading to a vinylphosphonium and copper nanoparticles.